

S. LAKÓ¹
J. SERES²
P. APAI¹
J. BALÁZS³
R.S. WINDELER⁴
R. SZIPŐCS^{1,5,✉}

Pulse compression of nanojoule pulses in the visible using microstructure optical fiber and dispersion compensation

¹ Research Institute for Solid State Physics and Optics, P.O. Box 49, Budapest 1525, Hungary

² Department of Physics, SzTE JGyTFK, 6725 Szeged, Boldogasszony sgt. 6, Hungary

³ Research Institute for Technical Physics and Material Science, P.O. Box 49, Budapest 1525, Hungary

⁴ OFS Fitel Laboratories, 600 Mountain Ave, Murray Hill, NJ 07974, USA

⁵ R&D Lézer-Optika Bt, P.O. Box 622, 1539 Budapest, Hungary

Received: 10 June 2002/Revised version: 15 November 2002
Published online: 12 February 2003 • © Springer-Verlag 2003

ABSTRACT Experimental results on the pulse compression of 1-nJ, 150-fs pulses from a tunable, 76-MHz Ti:sapphire laser oscillator operating at around 750 nm are reported. The length of the pulses can be compressed to nearly one tenth by applying a high-delta, single-mode microstructured optical fiber exhibiting zero group-delay dispersion at 767 nm, and by a prism-pair/chirped-mirror compressor. The experimental results are verified by theoretical investigations modeling the pulse propagation taking into account non-linear self-phase modulation and fiber dispersion.

PACS 42.65; 42.81

1 Introduction

Recent years have brought revolutionary progress in the generation and application of femtosecond laser pulses. One of the main directions of development is generating shorter and shorter laser pulses for laser spectroscopic investigations in the sub-10-fs time domain. With the invention of Ti:sapphire laser active media [1], Kerr-lens mode-locking [2] and chirped-mirror technology [3], it has become an everyday routine to generate sub-10-fs pulses: nowadays, such oscillators are available from several vendors, but their average output power and tunability are poor compared to commercial “100-fs” laser oscillators. From the practical point of view, it might be an important question whether it is possible to upgrade an existing 80–150-fs laser oscillator to a 10–30-fs one, since the price of such a short-pulse laser oscillator is still not negligible. There is an interest in pulse shortening possibilities in other technical fields as well [4]: laser oscillators used for optical communications exhibiting ultrahigh (~ 10 GHz) repetition rate cannot surpass the picosecond limit, although the broad spectrum is required for wavelength-multiplexing data transmission. Recently, pulse compression in the solitary-pulse-compression regime down to 54 fs was reported in dispersion-flattened optical fibers in the near-IR regime [4].

The first generation of commercial 100-fs Ti:sapphire pulse laser oscillators incorporates relatively long laser active

media (the path length is typically between 20 and 25 mm) with low doping concentrations, which are required for the broad tunability of these lasers: the lower the doping concentration (and the absorption at the pump wavelength) the higher the figure of merit (FOM) of the crystal. The dispersion of these relatively long crystals is typically compensated by a prism pair compressor (e.g. by an SF10 prism pair) exhibiting strong higher-order dispersion, limiting the minimum pulse duration of the laser at around 60 fs. By replacing the highly dispersive prism pair with lower dispersion prisms and increasing the prism separation, the pulse duration can be reduced to approximately 30 fs, although this modification changes the laser geometry considerably, requiring basic modifications to the laser mechanics. Another problem is the bandwidth of the one-element (1T) birefringent filter (BRF) used for the tuning of these lasers, which limits the laser bandwidth to 5–8 nm. Accordingly, the BRF must be replaced by a new BRF element supporting higher bandwidths.

In time-resolved spectroscopic studies, it would be desirable to work with femtosecond-pulse laser oscillators exhibiting broad tunability and a highly variable pulse duration (and spectral width) that do not require the changing of the cavity optics and mechanics. One possible, but rather expensive, solution is applying a kHz repetition rate, non-collinearly-phase-matched optical parametric amplifier pumped by the second-harmonic beam of a Ti:sapphire amplifier system [5]. In the case of more cost-effective fs-pulse laser oscillators, the first step to developing such a versatile system was the development of ultrabroadband chirped mirrors [6] for broadly tunable femtosecond-pulse Ti:sapphire laser oscillators, which exhibit high reflectivity and smooth group-delay versus wavelength functions over the bandwidth of 680 to 1060 nm [6]. (These mirrors are often referred to as “XBand optics” or “XWave optics”.) The pulse duration of Ti:sapphire oscillators incorporating XBand/XWave optics can still be varied in the 80 to 150-fs regime by adjusting intracavity dispersion. Further pulse shortening could be achieved by extracavity pulse compression [7], although the pulse energy (usually 1–10 nJ) and the corresponding light intensity of present day 100-fs laser oscillators are too low for efficient self-phase modulation in single mode, step-index fused silica optical fibers. The main problem is the rapid temporal broadening of the pulse due to chromatic dispersion, which reduces the peak power and thus the self-phase mod-

✉ Fax: +36-1/375-4553, E-mail: szipoecs@sunserv.kfki.hu

ulation over short distances in these optical fibers. In 1999, it was demonstrated for the first time that such high-delta microstructure optical fibers (MFs) can be constructed that exhibit zero chromatic dispersion within the tunability range of the most popular Ti:sapphire femtosecond-pulse laser oscillator [8]. Several non-linear phenomena, such as soliton propagation, second- and third-harmonic generation and continuum generation were demonstrated in these novel fibers with pulse energies below 1 nJ [8, 9]. For comparison, we must recall that in one of our previous experiments we required 35 to 50-nJ and 13-fs pulses for efficient spectral broadening supporting sub-5-fs pulses in a conventional step-index, single-mode optical fiber [10].

In this paper, the first theoretical and experimental results on spectral broadening and pulse compression in low-dispersion MF samples a few cm long, supplied with the combination of a prism pair and a chirped-mirror compressor, are reported. Based on our theoretical and experimental results, it is demonstrated that the set-up offers a nearly tenfold pulse shortening down to 15–18 fs at around 750 nm.

2 Theory

To describe pulse evolution in a microstructure optical fiber, the Fourier transform of the well-known space-time-dependent differential equation [11] was used, which is the reduced form of a system of equations describing femtosecond parametric oscillators [12]:

$$\begin{aligned} \frac{\partial^2 E(\omega, x)}{\partial x^2} = & -\frac{\omega^2 n^2(\omega)}{c^2} E(\omega, x) - \frac{\omega^2 \chi^{(3)}}{16\pi^3 c^2 w_0^2} \\ & \times \int_{-\infty}^{\infty} \left(\int_{-\infty}^{\infty} E(\omega', x) E^*(\omega' - \omega'', x) d\omega' \right) \\ & \times E(\omega - \omega'', x) d\omega'' . \end{aligned} \quad (1)$$

This equation takes into account the finite response time of the medium in the linear term and the self-phase modulation in the non-linear term. $E(\omega, x)$ denotes the spectral electric field (Fourier transform pair of the time-dependent electric field), $\chi^{(3)}$ is the third-order non-linear susceptibility in m/V^2 , and w_0 is the core radius ($0.85 \mu\text{m}$ [9]) assuming only one Gaussian TEM_{00} mode. (In our calculations, only this mode was considered, which is in accordance with our experimental conditions.) The factor before the convolution and cross-correlation integrals was calculated for this mode using the overlap integral of Gaussian modes [13, 14]. The refractive index $n(\omega)$ in our model requires special attention: besides the material dispersion, this function contains the waveguide dispersion contribution of the microstructure optical fiber. Unfortunately, this dispersion formula required for our calculations had not yet been measured for such a broad spectral range [8, 9]; we had to calculate it. We modified the material dispersion of bulk silica [11] after recognizing that the waveguide dispersion contribution is almost constant in the spectral range of interest (see Fig. 2 in [9]). This condition allowed us to write the refractive index of the fiber in the following form:

$$n(\lambda, \lambda_F) \approx n_{\text{FS}}(\lambda) - \left. \frac{dv_{\text{FS}}^{-1}(\lambda)}{d\lambda} \right|_{\lambda_F} c\lambda \ln \left[\frac{\lambda'(\lambda_F)}{\lambda} \right] \quad (2)$$

where $n(\lambda, \lambda_F)$ is the refractive index of the microstructure fiber with zero dispersion at λ_F , $n_{\text{FS}}(\lambda)$ and $v_{\text{FS}}(\lambda)$ are the refractive index and the group velocity of fused silica, respectively. This relation satisfies the boundary condition of the waveguide contribution, i.e. that it has to disappear at zero wavelength in the core. We approximated λ' as the double of the core diameter:

$$\lambda'(\lambda_F) \approx 2d_{\text{core}}(\lambda_F) \approx \frac{1.75}{\lambda_F^{-1} - \lambda_{\text{FS}}^{-1}}, \quad (3)$$

where λ_{FS} is the wavelength where the dispersion of fused silica is zero and the formula of the core diameter is approxi-

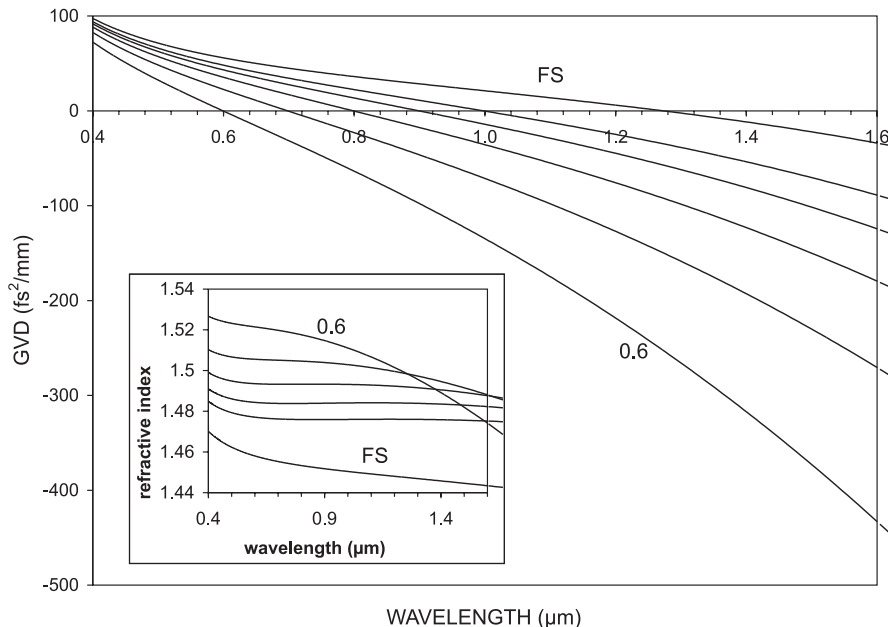


FIGURE 1 Calculated GVD and refractive index functions of microstructure optical fibers exhibiting different zero-dispersion wavelengths. (The curves corresponding to fused silica and MF samples with zero-dispersion wavelength of $0.6 \mu\text{m}$ are respectively labeled as FS and 0.6 in the figures.)

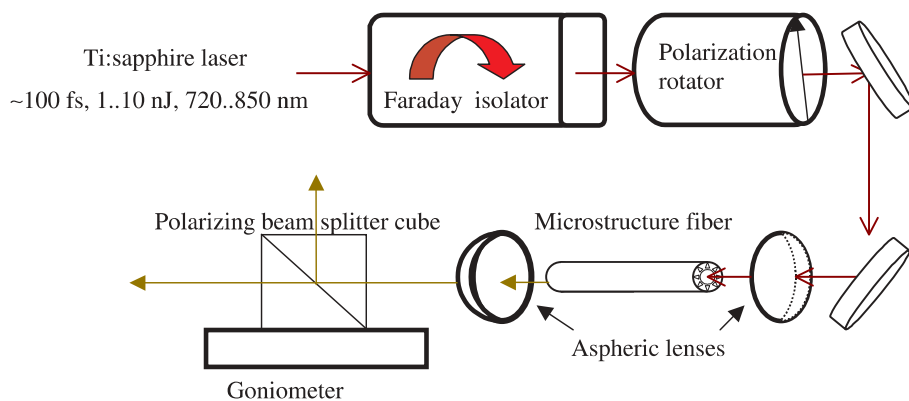


FIGURE 2 Experimental set-up for testing the optical properties of microstructure optical fiber samples

ated by the calculation of [9]. The factor of two was chosen to obtain the same behavior for the refractive index when previously measured [15]. The absorption is so low in the MF sample [15] that it can be neglected in our calculations. Calculated group velocity dispersion (GVD) functions and corresponding refractive indices (inset) of MF samples of different core diameters and that of bulk fused silica (FS) are shown in Fig. 1. We have to point out that (1) does not contain the slowly varying envelope approximation in the pulse propagation and the quasi-stationary approximation in the non-linear interaction. (These approximations must be avoided in the case of such broad spectra that we are currently working with.) We solved (1) numerically in the spectral domain by using 0.5-THz spectral and 2-nm spatial steps. The non-linear refractive index was chosen to be equal to that of bulk silica ($3 \times 10^{-20} \text{ m}^2/\text{W}$) according to the measurement described in [8]. In order to obtain the temporal pulse shapes, the computed spectra were inverse Fourier transformed.

The computed spectral intensity distributions of the self-phase-modulated (SPM) pulses as functions of the pump laser wavelength, the pulse energy and the fiber length were compared to our corresponding measured values for a number of different sets of parameters [16]. Although Raman effects play an important role in the later stage of supercontinuum generation [8], we found that our model provided a good description of the non-linear pulse propagation for fiber lengths up to several centimeters. In our current pulse compression experiments, we had to work with few-cm-long MF pieces, in which, due to Raman scattering, no shift of the SPM pulse spectrum could be observed, and the computed pulse spectra, taking into account exclusively self-phase modulation and dispersion, fit exactly to the corresponding measured spectral intensity functions [16]. Our experimental conditions aiming for pulse compression were determined by these numerical simulations, for which experiments will be discussed in the following section.

3 Experiments

As an initial step, we investigated the basic linear and non-linear optical properties of our MF samples. The experimental set-up for testing these optical properties is shown in Fig. 2. A tunable, mode-locked Ti:sapphire laser (FemtoRose 100 TUN laser, product of R&D Ultrafast Lasers Ltd.) is optically pumped by a 10 W multiline argon-ion laser

(Beamlock 2080 laser, product of Spectra Physics). The laser delivers mode-locked average output powers up to 800 mW at 8-W pumping. This average power, however, depends on the operation wavelength due to the wavelength-dependent gain of Ti:sapphire. During our studies, the operation wavelength was set between 720 and 850 nm by a BRF tuning element (1T quartz plate from VLOC Corp.). The BRF limits the spectral width at around 8 nm, hence the pulse duration at approximately 80 fs. The intracavity dispersion is controlled by adjusting the glass insertion of the SF 10 prism-pair compressor, resulting in 80 to 150-fs, nearly transform-limited pulses at the laser output. It is important to point out that the application of a Faraday isolator between the laser and the MF is required in order to avoid feedback from the backscattered light generated in the microstructure fiber. We found that the mode locking of the laser became very unstable without isolation. The Faraday isolator introduced a wavelength-dependent optical loss between 5 and 10%.

3.1 The effect of fiber polarization-mode dispersion

Our MF sample (drawn by OFS Fitel Laboratories) consisted of a 1.7- μm -diameter silica core surrounded by an array of 1.3 μm -diameter air holes in a hexagonal, closely packed arrangement (see Fig. 3) A small ellipticity in the fiber core lead to a polarization-maintaining birefringence [17].

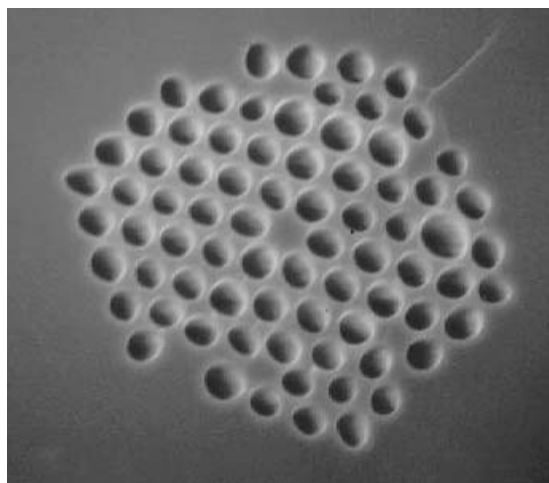


FIGURE 3 Electron micrograph image of the air-silica microstructure fiber

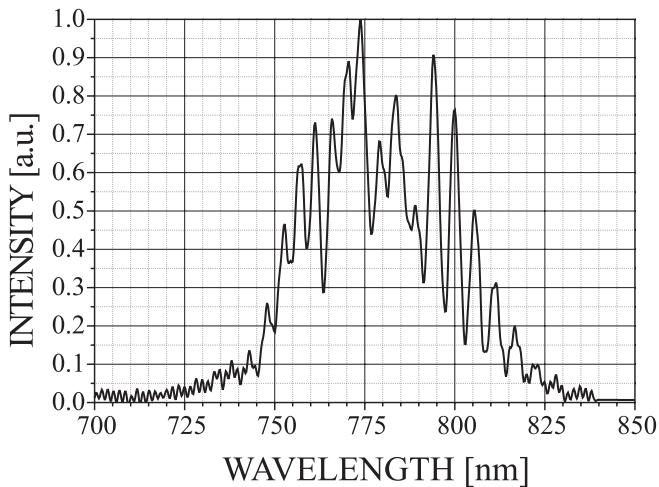
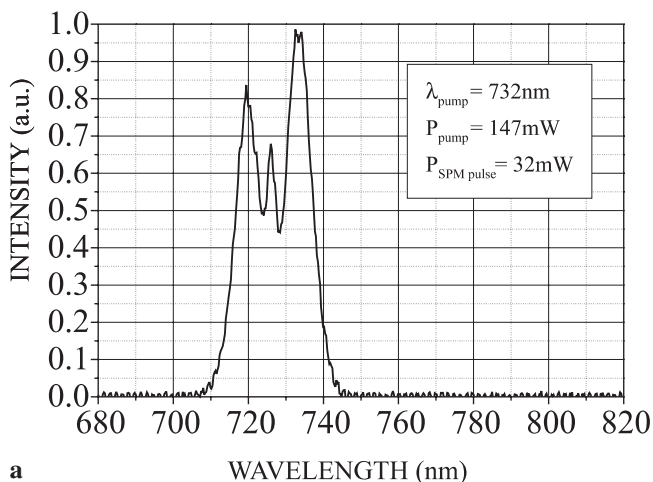


FIGURE 4 Spectral intensity distribution of two interfering self-phase-modulated pulses exiting the polarization-maintaining birefringent microstructure optical fiber. The analyzer was set to halfway (45°) between the polarization of the two pulses of orthogonal polarization

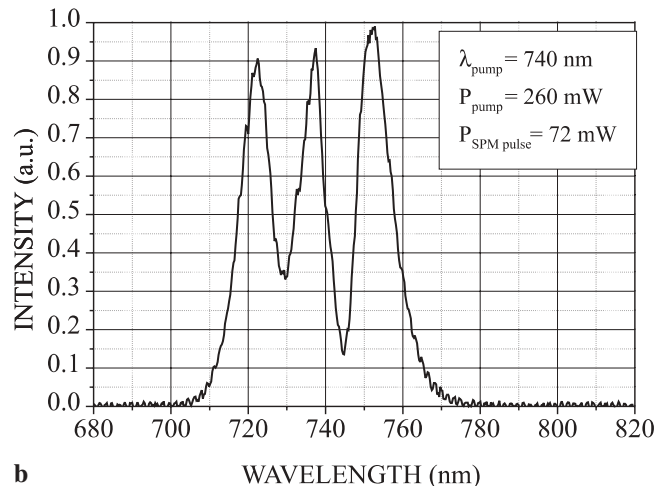
Accordingly, the polarization of the laser beam entering the optical fiber had to be properly set in order to generate a single (!) self-phase-modulated, i.e. spectrally broadened, pulse.

Otherwise, two different SPM optical pulses of orthogonal polarization were generated. In the latter case, the two SPM pulses exhibited different spectra and different propagation times through the optical fiber. Due to their orthogonal polarization, the two SPM pulses did not interfere. However, if an analyser was set at midway (45°) between the two polarization states, an interference effect could be observed in the measured intensity spectrum, as demonstrated in Fig. 4. For recording the spectrum shown in Fig. 4, optical pulses with central wavelengths of 750 nm were introduced to the MF sample.

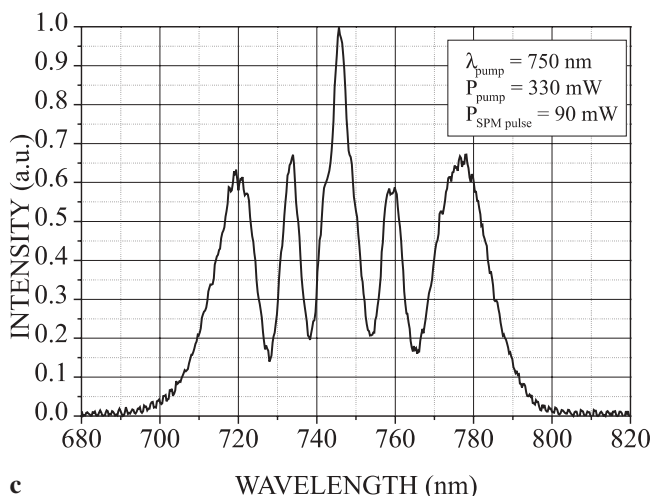
In our experiments aiming for pulse compression, the polarization of the laser beam entering the microstructure fiber was usually set by a polarization rotator (see Fig. 2). By adjusting the light polarization relative to the fiber's birefringent axis, we were able to generate single SPM pulses at the exit plane of the microstructure optical fiber. An anti-reflection-coated plastic aspheric lens ($N.A. = 0.45$, working distance $d = 1.9$ mm) was used for focusing our laser beam into the optical fiber. Coupling efficiencies measured between the focusing lens and the MF output were found in the 30%–35% range typically. The spectrally broadened output of the optical fiber was collimated by an achromatic microscope objective with $N.A. = 0.6$, or by a second low-dispersion aspheric lens.



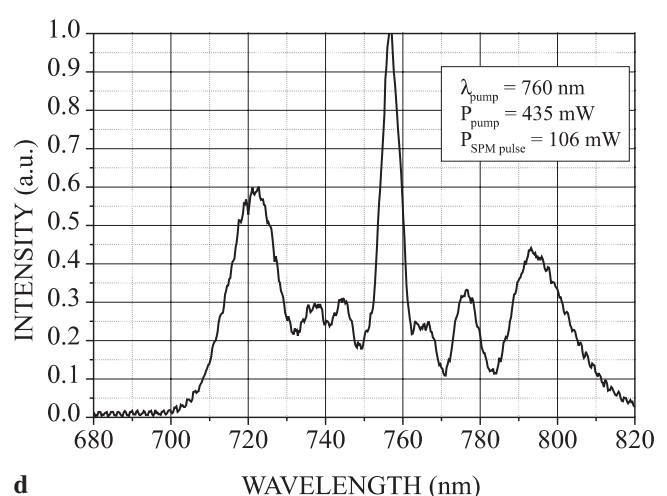
a



b



c



d

FIGURE 5 Spectral intensity distribution of the self-phase-modulated pulses exiting a 32-mm-long fiber at different laser wavelengths: **a** 732 nm; **b** 740 nm; **c** 750 nm; and **d** 760 nm

3.2 Optimizing laser and fiber parameters for compression

We investigated the spectral and temporal properties of the SPM pulses as functions of laser wavelength, chirp of the input pulse, energy of the pulse and the length of the microstructure optical fiber. The spectra were measured with a calibrated CCD-based spectrophotometer. After having performed a series of measurements and having obtained the first results of our computer simulations discussed above, we came to the conclusion that relatively short fiber pieces with lengths between 1 and 5 cm are best suited for pulse compression, while the laser operation wavelength must be set slightly below the zero-dispersion wavelength (767 nm) of the MF.

Typical SPM pulse spectra recorded for a microstructure fiber sample with a length of 32 mm and for different laser operation wavelengths are displayed in Fig. 5. Expecting that the self-phase-modulated pulses exiting the fiber have no residual chirp (in the case of ideal dispersion compensation), one can compute the (transformation-limited) temporal shape of the SPM pulses, as shown in Fig. 6. For instance, we found that the calculated FWHM pulse duration of the 750-nm pulse was approximately 15 fs (in the case of ideal dispersion compensation). In our current experiment we addressed the question of how far the pulse duration of a 100-fs laser Ti:sapphire oscillator can be reduced by means of spectral broadening in a piece of a microstructure optical fiber and by proper dispersion compensation. Hence the subsequent question to be answered is about the chirp of the SPM pulse exiting the fiber.

The spectral phase (chirp) of the SPM pulses were measured and compared to the computed values only for fewer sets of parameters (see later), due to the lack of a real-time device measuring the spectral phase directly. However, considering the fact that spectral broadening due to self-phase modulation is determined by the temporal shape of the propagating pulse, we could expect that if the spectral intensity distribution functions of the SPM pulses computed for different fiber lengths and pulse energies agree with the corresponding measured

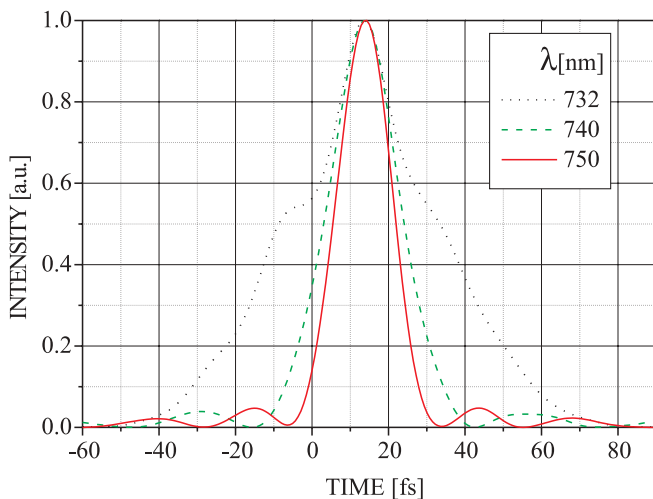


FIGURE 6 Computed temporal pulse shape of transform-limited optical pulses corresponding to the spectra shown in Fig. 5: 732 nm (dotted); 740 nm (dashed); and 750 nm (continuous line)

values, the same would apply for the computed spectral phase (chirp).

In order to determine the best experimental conditions for producing the broadest spectrum and still compressible SPM pulses (referred to as “best” below), a series of calculations was performed based on the model described in Sect. 2. During our calculations, the zero-dispersion wavelength of the fiber was varied, and the input pulse energy, central wavelength, pulse duration and pre-chirp were chosen as 1 nJ, 750 nm, 150 fs and 5000 fs², respectively. The calculations were performed for propagation distances up to 10 cm. The computed best spectra as a function of zero-dispersion wavelength are presented in the insets of Fig. 7, along with the corresponding optimum fiber lengths. These values are indicated next to every computed spectrum, together with the dispersion-compensated (up to the second order) temporal pulse shapes as insets.

The calculation predicts a well-compressible and short pulse only if the input pulse and the full spectrum of the SPM pulse are in the positive dispersion range of the fiber. In this case, the full SPM spectrum contains a positive linear chirp, which can be well compensated with the combination of low-loss, negative dispersion, discrete optical elements such as prism pairs and chirped mirrors [18, 19]. In the case when the zero-dispersion wavelength is equal to or near the wavelength of the input pulse (in our models this wavelength is 750 nm), the output spectrum is split into two parts; one with positive and one with negative chirp. Accordingly, we obtained a double pulse, a short one and a long one in the time domain, depending on which spectral part was dispersion compensated (see insets in Fig. 7). This was experimentally proved after generating a broad spectrum extending from 700 to 820 nm: we were able to compress the spectral components of the SPM pulses in the negative and the positive dispersion regimes separately close to the transform limit if we shaded the unwanted spectral components in our prism-pair compressor. However, very different prism adjustments were required for the spectral components below and above the zero-dispersion wavelengths in order to obtain the shortest autocorrelation traces.

In the negative dispersion regime of the MF, the spectrum was divided into two negatively chirped parts that propagated at different group velocities. Thus we obtained a double pulse again, but both of them were dispersion compensated. This explains the large difference between the linearly and ideally dispersion-compensated pulse duration in this regime in Fig. 7. This latter observation can be attributed to the solitary pulse formation in the negative dispersion regime.

Concluding the results of our experimental and theoretical investigations described above, we can say that relatively short, few-cm-long fiber pieces are the most useful for pulse compression, while the laser operation wavelength must be set below the zero-dispersion wavelength (767 nm) of the MF in such a way that the full spectrum of the SPM pulse has to be in the positive dispersion range. Unfortunately, the spectral broadening of the SPM pulse was limited at shorter wavelengths due to the reduced output power of our tunable Ti:sapphire laser oscillator, which ultimately limited the performance (pulse shortening capabilities) of our present pulse-compression scheme.

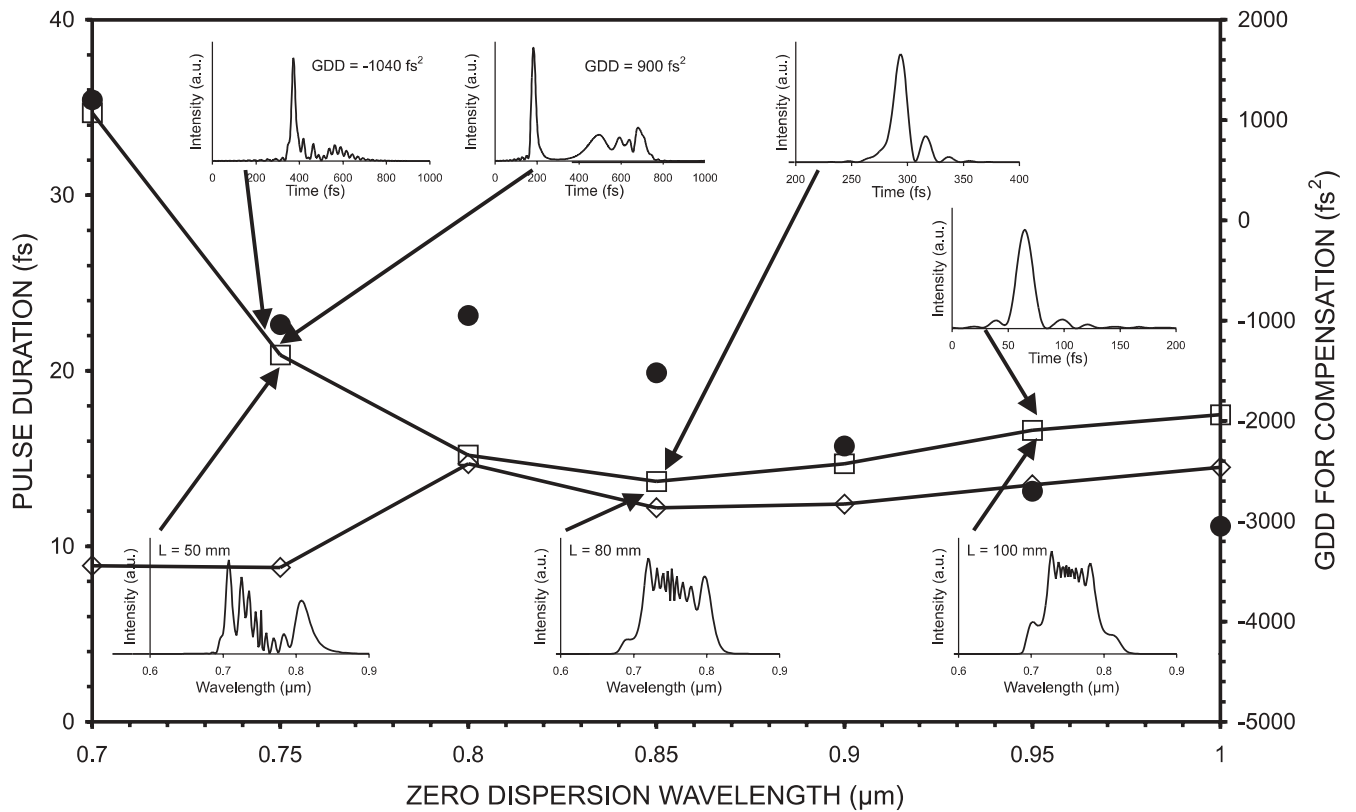


FIGURE 7 Calculated pulse duration of SPM pulses in the case of best linear (*square*), ideal (*diamond*) chirp compensation in microstructure optical fibers with various zero-dispersion wavelengths, and the necessary GDD compensation (*filled circle*). The *insets* show a few corresponding computed spectra and temporal pulse shapes

3.3 Chirp measurement and dispersion compensation

The chirp of our SPM pulses was measured by sum-frequency generation (SFG): we coupled out approxi-

mately 15% of the laser output by a beamsplitter (gating pulse) and the rest of the energy was introduced into the optical fiber, which generated the SPM pulse (see Fig. 8). The sum frequency of the SPM pulse and the gating pulse was gener-

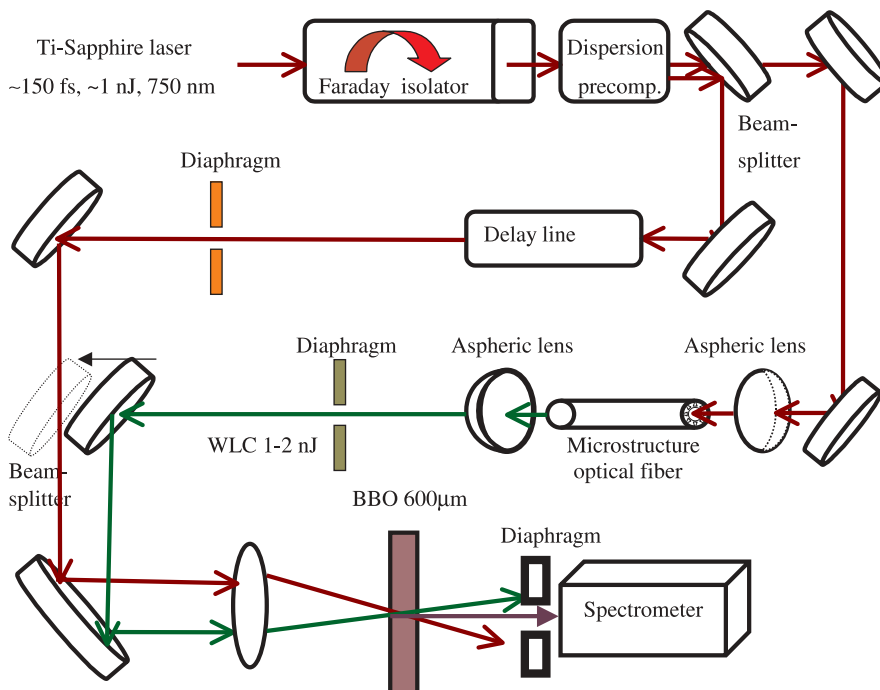


FIGURE 8 Experimental set-up for measuring the temporal chirp of the self-phase-modulated optical pulses by sum-frequency generation in a 600- μm -thick BBO crystal

ated in a 600- μm -thick BBO crystal, the orientation of which was always set for a maximum SFG signal. The angle between the SPM pulse and the gating pulse was set to approximately 5° in the BBO crystal, which corresponded to approximately 8° outside the crystal. The result of the chirp measurement in the case of the 750-nm SPM pulse is shown in Fig. 9. After the evaluation of our measured data, we determined that the SPM pulse exhibited a nearly linear positive chirp of approximately 1000 fs^2 at 750 nm.

In connection with dispersion compensation, we have to mention that our Faraday isolator exhibited a relatively high dispersion, which had to be balanced in the normal dispersion regime of our optical fiber samples for efficient self-phase modulation (i.e. spectral broadening). For this purpose, the laser output passed an SF 10 prism-pair (pre)compressor for optimizing the chirp of the femtosecond pulse entering the microstructure optical fiber. The prism separation was set to approximately 44 cm, being determined by the measured dispersion of our Faraday isolator.

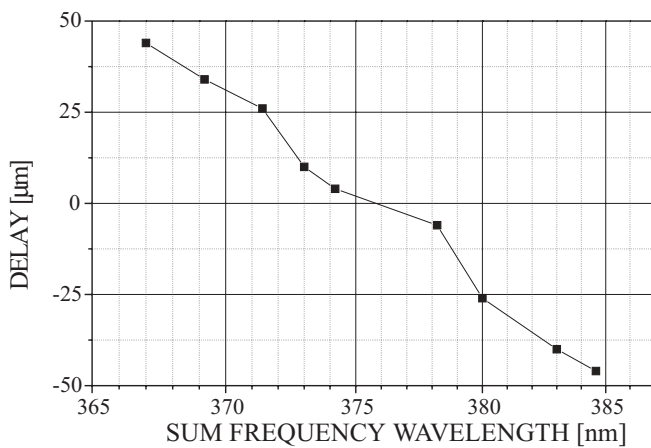


FIGURE 9 Group delay vs. sum-frequency central wavelength corresponding to a spectrally broadened pulse exiting the fiber measured by the set-up shown in Fig. 6 (pump wavelength: 750 nm, fiber length: $L = 32 \text{ mm}$, pulse energy: $\sim 1 \text{ nJ}$)

Concerning the chirp of the SPM pulse, there are two possible solutions for compensating this linear chirp: using a pure chirped-mirror (CM) compressor [19] or a combined prism-pair/chirped-mirror compressor [18]. The former solution has the advantage of easier use, but requires chirped mirrors with very low oscillation in their group delay vs frequency functions due to the relatively high number of reflections (25 reflections in the case of a CM exhibiting a typical group delay dispersion (GDD) of -40 fs^2 per reflection) required for compensating such a high positive dispersion. We recently reported on such mirror designs [19] exhibiting a GDD of $-50 \pm 1 \text{ fs}^2$ over the wavelength regime of 740 to 860 nm, which were successfully adopted for tunable 100-fs Ti:sapphire laser oscillators. However, the SPM spectrum generated with our 750-nm laser pulses did not fit the negative GDD regime of the above-mentioned chirped mirrors, hence a new CM design with an unusual operation regime has to be manufactured for such a compact pulse compressor. An alternative solution is to use a prism-pair/chirped-mirror compressor designed for sub-10-fs Ti:sapphire laser oscillators and laser amplifiers [18]: a fused silica prism pair provides the required relatively high negative GDD, while CMs compensate for the negative third-order dispersion (TOD) of the prism-pair compressor. In these pulse-compression experiments, we chose the latter approach in order to have more flexibility in our dispersion compensation scheme, allowing us to set not only the GDD but the TOD as well.

The temporal shape of the compressed SPM pulses was measured by recording the corresponding second-order interferometric autocorrelation traces with a 2-photon detector (a green LED) or by the use of a 15- μm -thick BBO crystal and a PMT detector (see Fig. 10). A measured interferometric autocorrelation trace corresponding to a slightly chirped 750-nm SPM pulse is shown in Fig. 11a. A nearly constant negative GDD of -910 fs^2 was provided for compensating the chirp of the spectrally broadened optical pulse of a fused silica prism pair exhibiting a negative GDD of -770 fs^2 and a negative TOD of -1500 fs^3 , and of a pair of chirped mirrors with negative GDD of -140 fs^2 and a positive TOD of 1600 fs^3

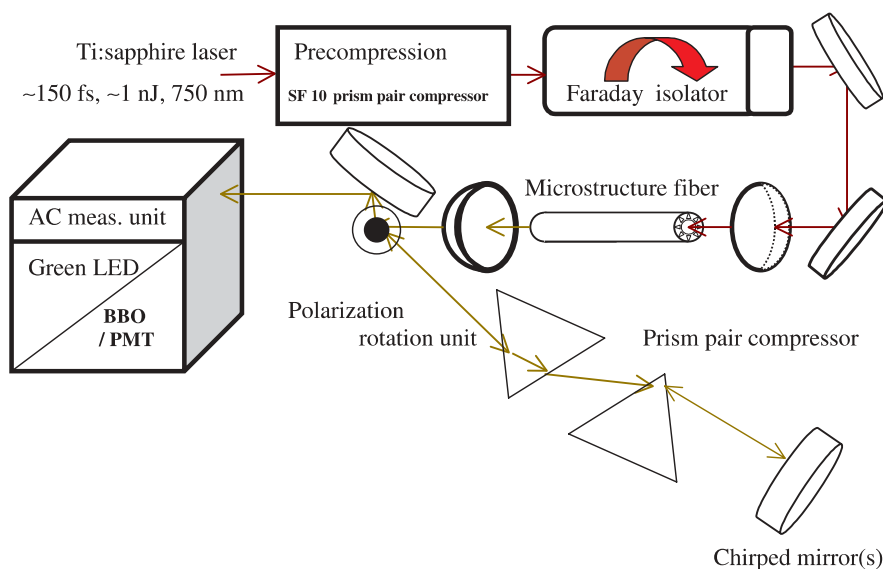


FIGURE 10 Experimental set-up used for pulse compression. A fused silica prism-pair compressor combined with chirped mirrors is used to compensate the positive chirp of the spectrally broadened optical pulses. The temporal shape of the compressed pulses are characterized by an interferometric second-order autocorrelator

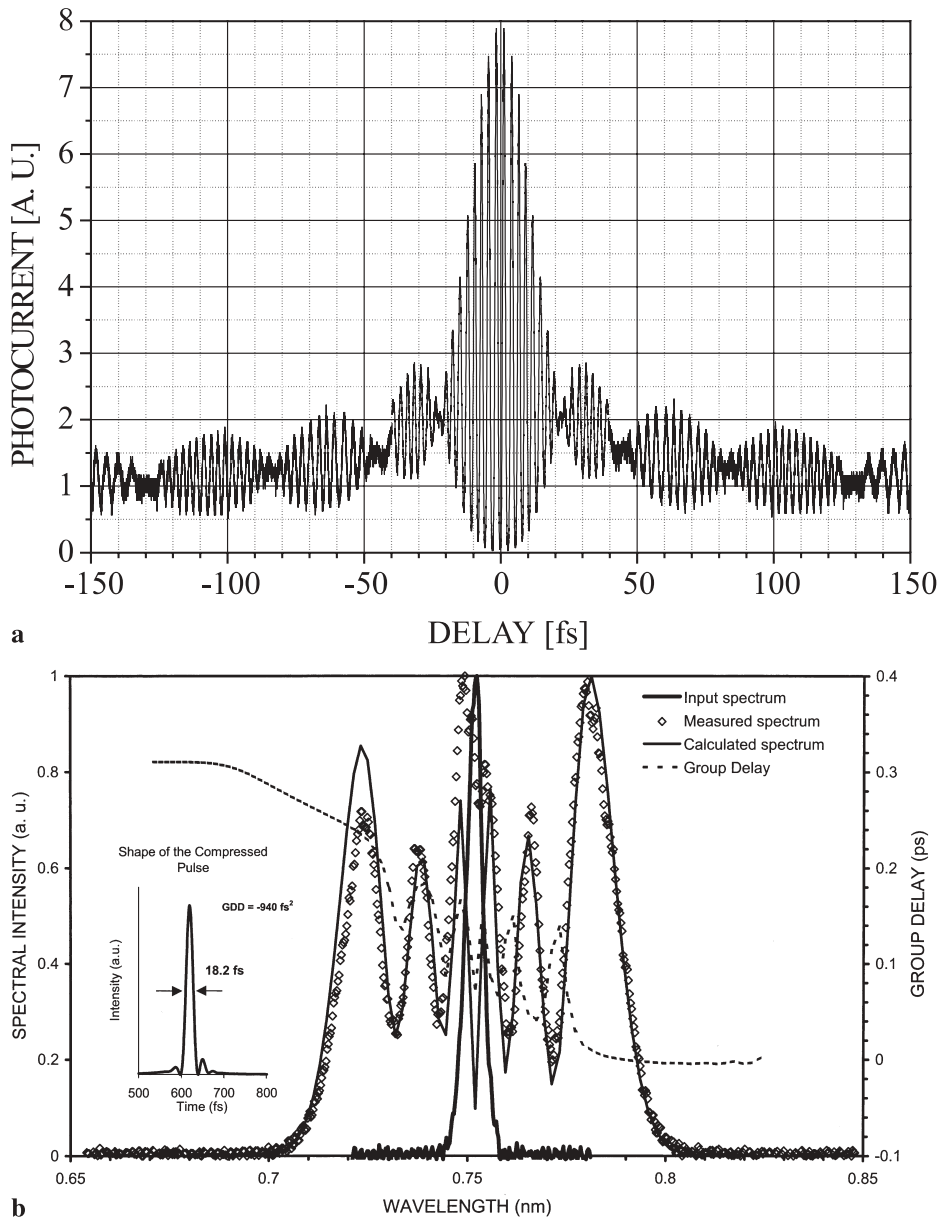


FIGURE 11 Measured interferometric autocorrelation trace (a) and the corresponding computed spectrum and group delay (b) compared with the measured spectrum. The *inset* shows the temporal intensity profile of a slightly chirped compressed 750-nm pulse

(upon four reflections). The required measure of GDD compensation is in good agreement with the calculated value of -940 fs^2 , which was obtained by computer modeling of the non-linear pulse propagation in the MF (see Fig. 11b). In the case of the dispersion-compensation stage described above, the calculated spectrum (which was also in perfect agreement with the measured one) and the residual phase error resulted in optical pulses with duration of 18.2 fs (see inset of Fig. 11b). This is very close to the transform-limited value of 18.1 fs, which corresponds to the case of ideal dispersion compensation. The measured pulse duration, however, was slightly longer (approximately 23–25 fs), which can be attributed to the non-ideal higher-order dispersion compensation in this experiment: our spectrum extends down to 680 nm, which is out of the typical specification bandwidth of our chirped mirrors designed for higher-order dispersion compensation in prism-pair-controlled Ti:sapphire laser oscillators.

The main limiting factor in our pulse compression experiment, however, was the fact that the MF sample had its zero-dispersion wavelength at 767 nm, which did not fit the gain maxima of our Ti:sapphire laser oscillator at around 790 nm: we found that for stable pulse compression we had to work in the positive- (normal) dispersion regime of the fiber, i.e. below 767 nm, where the output power of our laser was considerably lower and this set a limit on the spectral broadening of the pulse.

4 Conclusion

We have shown that the pulse duration of 100-fs laser oscillators with pulse energies in the few-nJ regime can be considerably reduced by applying a piece of microstructure optical fiber a few cm long and a prism-pair/chirped-mirror compressor. In our experiment, the microstructure optical fiber had its zero-dispersion wavelength at 767 nm and

a strong wavelength dependence of the dispersion around this wavelength (a strong cubic dispersion), which were the main limiting factors in reducing the pulse duration in our present pulse-compression scheme. Based on our computer simulations, we can say that dispersion-flattened microstructure fibers exhibiting low positive dispersions around the gain maxima of the most common 100-fs laser sources would offer the possibility of further pulse shortening of the nJ pulses of these laser oscillators.

ACKNOWLEDGEMENTS J. Seres thanks E. Seres for her valuable help in the computer simulations, R. Szipőcs thanks M. Serényi for advice regarding handling the optical fiber samples. This work was supported by the Hungarian Science Foundation under Contract Nos. OTKA-T029578, NKFP3-00164/2001, by Széchenyi NRP and by R&D Lézer-Optika Bt.

REFERENCES

- 1 P.F. Moulton: *J. Opt. Soc. Am. B* **3**, 125 (1986)
- 2 D.E. Spence, P.N. Kean, W. Sibbett: *Opt. Lett.* **16**, 42 (1991)
- 3 R. Szipőcs, K. Ferencz, C. Spielmann, F. Krausz: *Opt. Lett.* **19**, 201 (1994)
- 4 K.R. Tamura, M. Nakazawa: *Opt. Lett.* **26**, 762 (2001)
- 5 A. Shirakawa, I. Sakane, T. Kobayashi: *Ultrafast Phenomena XI* (Springer, Heidelberg, Berlin 1998) p. 54
- 6 E.J. Mayer, J. Möbius, A. Euteneuer, W.W. Rühle, R. Szipőcs: *Opt. Lett.* **22**, 528 (1997)
- 7 R.L. Fork, C.H. Brito Cruz, P.C. Becker, C.V. Shank: *Opt. Lett.* **12**, 483 (1987)
- 8 J.K. Ranka, R.S. Windeler, A.J. Stentz: *Opt. Lett.* **25**, 25 (2000)
- 9 J.K. Ranka, R.S. Windeler, A.J. Stentz: *Opt. Lett.* **25**, 796 (2000)
- 10 A. Baltuska, Z. Wei, M.S. Pshenichnikov, D.A. Wiersma, R. Szipőcs: *Appl. Phys. B* **65**, 175 (1997)
- 11 G.P. Agrawal: *Non-Linear Fiber Optics* (Academic Press, Inc., San Diego, CA 1989)
- 12 J. Seres, J. Hebling: *J. Opt. Soc. Am. B* **17**, 741 (2000)
- 13 G. Görer, R. Laenen: *Opt. Commun.* **152**, 429 (1998)
- 14 C. Schwob, P.F. Cohadon, C. Fabre, M.A.M. Marte, H. Ritsch, A. Gatti, L. Lugiato: *Appl. Phys. B* **66**, 685 (1998)
- 15 T.P. White, R.C. McPhedran, C.M. de Sterke, L.C. Botten, M.J. Steel: *Opt. Lett.* **26**, 1660 (2001)
- 16 R. Szipőcs, S. Lakó, P. Apai, J. Seres, R.S. Windeler: Paper SMR.1397-9, Winter College on Ultrafast Non-linear Optics, Trieste, Italy, 18 February–1 March 2002 (ICTP, Trieste 2002)
- 17 G. Millot, A. Sauter, J.M. Dudley, L. Provino, R.S. Windeler: *Opt. Lett.* **27**, 695 (2002)
- 18 C. Spielmann, M. Lenzner, F. Krausz, R. Szipőcs: *Opt. Commun.* **120**, 321 (1995)
- 19 R. Szipőcs, A. Köházi-Kis, S. Lakó, P. Apai, A.P. Kovács, G. DeBell, L. Mott, A.W. Louderback, A.V. Tikhonravov, M.K. Trubetskov: *Appl. Phys. B* **70**, S51 (2000)